Assays of vacuole fusion resolve the stages of docking, lipid mixing, and content mixing

Youngsoo Jun and William Wickner*

Department of Biochemistry, Dartmouth Medical School, Hanover, NH 03755

Edited by Peter Novick, Yale University, New Haven, CT, and accepted by the Editorial Board June 30, 2007 (received for review February 1, 2007)

Membrane fusion entails organelle docking and subsequent mixing of membrane bilayers and luminal compartments. We now present an *in vitro* assay of fusion, using yeast vacuoles bearing domains of either Fos or Jun fused to complementary halves of β-lactamase. Upon fusion, these proteins associate to yield β-lactamase activity. This assay complements the standard fusion assay (activation of pro-Pho8p in protease-deficient vacuoles by proteases from *pho8*Δ vacuoles). Both the β-lactamase and pro-Pho8p activation assays of fusion show the same long kinetic delay between SNARE pairing and luminal compartment mixing. Lipid-mixing occurs rapidly after SNARE pairing but well before aqueous compartment mixing. These results support a model in which SNARE pairing leads to rapid hemifusion, followed by slow further lipid rearrangement and aqueous compartment mixing.

GTPγS | hemifusion | membrane fusion | SNARE | yeast vacuole

Yeast vacuole homotypic fusion occurs in several stages. During priming, Sec18p (NSF) and Sec17p disassemble *cis*-SNARE complexes, releasing Sec17p and the soluble SNARE Vam7p. Vacuole tethering is mediated by the Ypt7p Rab GTPase and its effector complex HOPS. Fusion proteins and regulatory lipids (diacylglycerol, phosphoinositides, and ergosterol) are concentrated at a ring-shaped microdomain, the "vertex ring," surrounding the apposed membranes of docked vacuoles. During docking, the released Vam7p rebinds to the vacuole through its affinities for phosphatidylinositol 3-phosphate (1) and HOPS (2) and participates in the formation of *trans*-SNARE complexes between apposed vacuolar membranes. Bilayer fusion around the vertex ring permits lipid and aqueous compartment mixing. It has been proposed that membrane fusion may require a lipidic "hemifusion" intermediate, where the closely apposed membrane leaflets are fused and mix, whereas the distal leaflets and aqueous compartments remain distinct. Hemifusion has been directly observed with influenza HA (3–5), either wild-type or with a GPI-anchor in place of its transmembrane domain (TMD), in a minimal SNARE-driven liposome fusion system (6, 7) with low levels of wild-type SNARE proteins or with mutant SNARE proteins with partial TMDs that span only one bilayer leaflet (6). Hemifusion was also observed in cell–cell fusion mediated by GPI-anchored SNARE proteins expressed on the outer surface of the plasma membrane (8), suggesting that all SNARE-dependent fusion might proceed by means of hemifusion. A hemifusion intermediate was proposed for yeast vacuole fusion, based on the finding that GTPγS allows lipid mixing while blocking the fusion-dependent activation of pro-Pho8p (9). The standard *in vitro* assay of vacuole fusion measures the proteolytic activation of the inactive pro-Pho8p (alkaline phosphatase or ALP) by vacuolar proteases upon content mixing between two populations of vacuoles. One limitation of this assay is its sensitivity to reagents that inhibit the activation of ALP. We have therefore developed an *in vitro* assay of yeast vacuole fusion in which content mixing between two vacuole populations is measured by the reconstitution of active *Escherichia coli* TEM-1 β-lactamase from two complementary fragments of the enzyme, each contributed from distinct vacuole populations. This fusion assay, coupled with a lipid mixing assay, has revealed that docking and lipid mixing are completed long before luminal contents mix. The kinetic gap between lipid and content mixing suggests that vacuoles fuse via a hemifusion intermediate, although we have not directly observed hemifusion structures.

Results

The standard *in vitro* vacuole fusion assay requires vacuoles from two strains. One lacks the proteases that activate vacuolar enzymes and contains only the catalytically inactive form of Pho8p (proALP). The other strain has vacuolar proteases but is deleted for the *PHO8* gene. Fusion allows the proteases to gain access to the inactive proALP and form active ALP. This assay has the intrinsic limitation of sensitivity to any reagent that inhibits ALP activity, the formation of active ALP, or vacuolar proteases. We have therefore developed a complementary fusion (content mixing) assay that does not require ALP or proteases. This assay, based on the studies of Blau and colleagues (10), uses vacuoles from two yeast strains (Fig. 1*A*). One contains a chimeric protein of three parts: a fragment of carboxypeptidase Y (CPY) specifying vacuole targeting (11), the α197 fragment of the *E. coli* TEM-1 β-lactamase, and the leucine zipper helix from c-Jun (α-Jun). The other carries a fusion protein of the same domain of CPY, the ω198 fragment of β-lactamase, and the leucine zipper helix from c-Fos (Fos-ω). Although neither population of vacuoles [supporting information (SI) Fig. 5*A*] has β-lactamase activity (Fig. 1*B*, diamonds and squares), fusion allows luminal protein mixing and rapid heterodimerization of Fos and Jun helices, which brings the α197 and ω198 fragments together to reconstitute β-lactamase activity (Fig. 1*B*, circles). This assay (hereafter termed the β-lactamase assay) complements the ALP fusion assay: (*i*) No orthologs of β-lactamase have been found in eukaryotes, including *Saccharomyces cerevisiae*, and thus the assay may avoid background activities. (*ii*) Yeast vacuolar proteases can be released by lysis during *in vitro* incubations and interfere with biochemical analysis. The β-lactamase assay uses only protease-deficient vacuoles. (*iii*) Although phosphorylation and proteolysis can regulate trafficking, phosphatase or protease inhibitors may inhibit the ALP assay itself. The β-lactamase fusion assay allows facile study of the roles of phosphorylation or proteolysis in vacuole fusion. The β-lactamase and ALP assays measure luminal compartment

Author contributions: Y.J. and W.W. designed research; Y.J. performed research; Y.J. and W.W. analyzed data; and Y.J. and W.W. wrote the paper.

The authors declare no conflict of interest.

This article is a PNAS Direct Submission. P.N. is a guest editor invited by the Editorial Board.

Abbreviations: MED, myristoylated alanine-rich C-kinase substrate (MARCKS) effector domain; CPY, carboxypeptidase Y; ALP, alkaline phosphatase; HOPS, homotypic vacuole fusion and vacuole protein sorting.

*To whom correspondence should be addressed at: Department of Biochemistry, Dartmouth Medical School, 7200 Vail Building, Hanover, NH 03755-3844. E-mail: bill.wickner@dartmouth.edu.

This article contains supporting information online at www.pnas.org/cgi/content/full/0700970104/DC1.

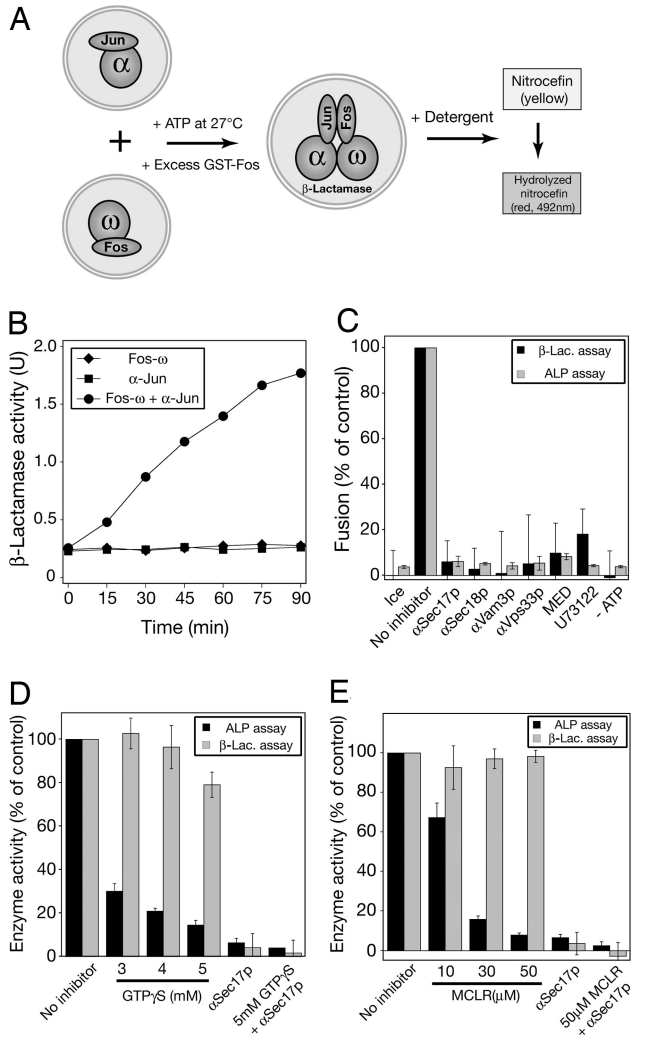

Fig. 1. A vacuole fusion assay. (*A*) An *in vitro* vacuole fusion assay based on complementary reconstitution of β-lactamase. (*B*) Fusion-dependent β-lactamase activity formation over the 90-min time course. BJ3505-Fos-ω vacuoles, BJ3505-α-Jun vacuoles, or both were incubated at 27°C in fusion reactions. A portion of reactions was transferred to ice at indicated times and assayed for β-lactamase activity. One unit (U) of the β-lactamase activity is defined as 1 nmol of hydrolyzed nitrocefin per min from 12 μg of vacuole protein. (*C*) Comparison between the β-lactamase (black bars) and ALP (gray bars) fusion assays. Fusion reactions (see *Materials and Methods*) were incubated for 90 min on ice or at 27°C with indicated inhibitors. One reaction lacked ATP. Values were normalized to the reactions without inhibitors (3.78 ± 0.65 units for the ALP assay; 1.76 ± 0.45 units for the β-lactamase assay). Data represent mean ± SEM ($n = 3$). Inhibitors concentrations: affinity-purified anti-Sec17p (153 nM), affinity-purified anti-Sec18p (142 nM), anti-Vam3p IgG (444 nM), affinity-purified anti-Vps33p (155 nM), MED (10 μM), and U73122 (60 μM). (*D* and *E*) The β-lactamase fusion assay is less sensitive to microcystin-LR (MCLR) and GTPγS than the ALP assay. The β-lactamase (gray bars) and the ALP (black bars) fusion assays were performed in the presence of increasing concentrations of GTPγS (*D*) or MCLR (*E*) and antibodies to Sec17p where indicated. Values were normalized to the reactions without inhibitors (4.6 ± 0.38 units for the ALP assay; 1.74 ± 0.27 units for the β-lactamase assay). Data represent mean ± SEM ($n = 3$).

mixing; each will be sensitive to inhibitors of fusion or of the maturation or catalytic activity of its respective reporter enzyme.

To determine whether the β-lactamase assay monitors Rab- and SNARE-dependent vacuole fusion, we compared the effects of known fusion inhibitors on the β-lactamase and ALP assays (Fig. 1*C*). Expression of the vacuole-targeted α-Jun or Fos-ω helical domains *per se* did not affect fusion, because vacuoles from BJ3505-α-Jun or BJ3505-Fos-ω fused with DKY6281 vacuoles just as well as BJ3505 vacuoles (data not shown). Fusion in both assays requires ATP and was blocked by priming inhibitors such as antibodies to Sec17p or Sec18p, docking inhibitors such antibodies to Vam3p or Vps33p, and lipid modifiers such as the MED peptide that binds to phosphoinositides and the PLC inhibitor U73122. Thus the β-lactamase assay measures authentic vacuole fusion. However, microcystin-LR (MCLR) and the nonhydrolyzable GTP analogue GTPγS, previously reported as fusion reaction inhibitors (12, 13), showed different inhibitory effects (Fig. 1 *D* and *E*). The β-lactamase assay was less sensitive to MCLR or GTPγS than the ALP assay. Neither MCLR nor GTPγS alone increases β-lactamase activity in a fusion-independent manner, as the development of β-lactamase activity seen with 5 mM GTPγS or 50 μM MCLR is fully sensitive to antibodies to Sec17p. The formation of β-lactamase activity in mixed detergent lysates of BJ3505-α-Jun or BJ3505-Fos-ω vacuoles is little affected by 5 mM GTPγS or 100 μM MCLR (see SI Fig. 5*C*). MCLR prevents the development of active ALP in mixed detergent lysates of BJ3505 and DKY6281 vacuoles (SI Fig. 6*A*, triangles) even though it permits substantial proteolytic formation of ALP from pro-ALP with intact vacuoles, a hallmark of fusion (SI Fig. 6*B*, lane 6). Thus, MCLR has greater potency to inhibit the ALP assay than to prevent *in vitro* vacuole fusion. Because higher concentrations of GTPγS showed some inhibition of the β-lactamase assay (Fig. 1*D*), we further explored GTPγS inhibition. Vacuoles from BJ3505 or DKY6281 were solubilized in Triton X-100, incubated separately in the absence or presence of 5 mM GTPγS on ice, and, after 20 min, mixed and incubated at 27°C. GTPγS (5 mM) partially (< 50%) blocked the proteolytic cleavage of pro-ALP in detergent (SI Fig. 6*B*, lane 5 vs. lane 4) and completely prevented the development of ALP activity (SI Fig. 6*A*, squares). The slow rate of pro-ALP maturation in this experiment likely reflects the large dilution of the proteases upon lysis as compared with their high concentrations within intact vacuoles. Thus GTPγS inhibits pro-ALP cleavage or ALP activation more than it inhibits fusion *per se*. To further explore this, fusion reactions with intact vacuoles were incubated for 90 min under low Mg^{2+} conditions, where the ALP assay is more sensitive to GTPγS, and were assayed for ALP activity (SI Fig. 6*D*) or for the proteolytic maturation of pro-ALP by immunoblotting (SI Fig. 6 *C* and *D*). High concentrations of GTPγS prevent the proteolytic maturation of pro-ALP. Although 2 mM GTPγS reduced the proteolytic maturation of pro-ALP by only 15%, the ALP activity was reduced by 80% (SI Fig. 6*D*). These data show that low concentrations of GTPγS can inhibit the ALP assay by preventing the development of the active form of the enzyme; they do not distinguish whether higher concentrations inhibit fusion or merely block the proteolytic maturation of pro-Pho8p. We therefore examined the effects of GTPγS by measuring the fusion-dependent size increase of vacuoles (Fig. 2). Vacuoles were incubated on ice or at 27°C, without inhibitor or with GTPγS or Fab fragments of antibody to Sec18p, and were then labeled with the lipophilic dye MDY-64 and observed by fluorescence microscopy. Although many large vacuoles were formed in a standard reaction (Fig. 2*B*), no large vacuoles were formed on ice (Fig. 2*A*) or in reactions with antibodies to Sec18p (Fig. 2*C*). As many large vacuoles were seen in a reaction with 4 mM GTPγS (Fig. 2*D*) as in the reaction without inhibitor (Fig. 2*B*), although the development of ALP activity was 80% inhibited (Fig. 2*G*). The fusion-dependent size increase of vacuoles in the presence of 4 mM GTPγS is indistinguishable from that of the reaction without inhibitors (Fig. 2*F*). Vacuole clustering and fusion began to be inhibited by 5 mM GTPγS (Fig. 2*E*). Large vacuoles are a particularly clear sign of vacuole fusion (Fig. 2*F*). Whereas 86 vacuoles acquired >60 μm^2 surface area through fusion in a

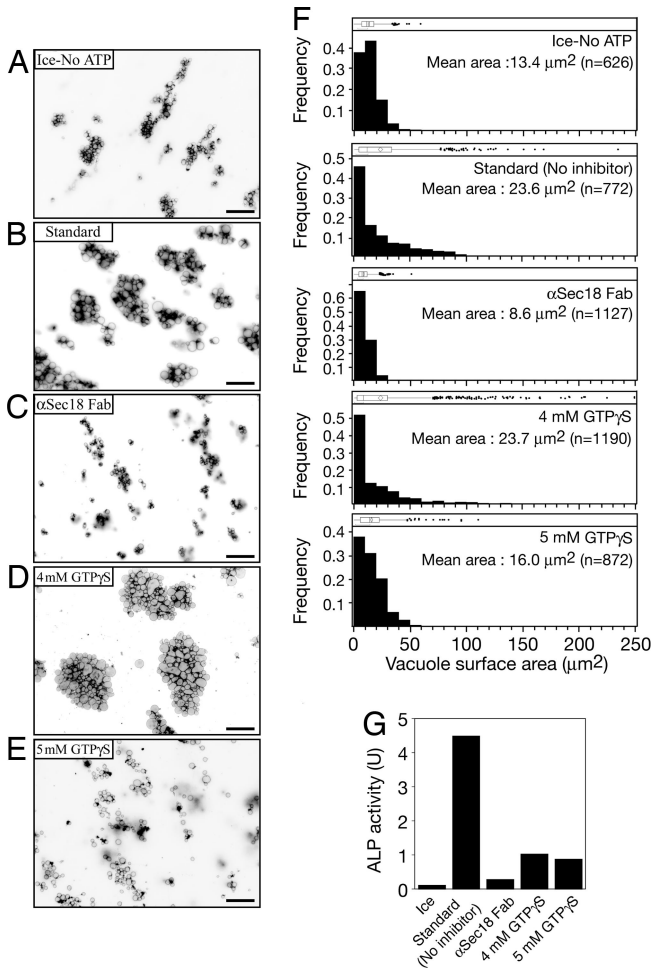

Fig. 2. GTPγS allows fusion but prevents pro-ALP activation. Fusion reactions were performed under standard conditions but with 10 μg of vacuoles. After 90 min, aliquots were stained with 3.3 μM MDY-64 for fluorescent microscopy (*A–F*) or assayed for ALP activity (*G*). Images were acquired and analyzed by using ImageJ 1.36b and JMP 5.0.1a (SAS Institute). Vacuole diameters were measured from micrographs taken from random fields, and the surface areas of individual vacuoles were plotted as distribution histograms (*F*). A representative field for each condition is shown (Scale bars, 20 μm).

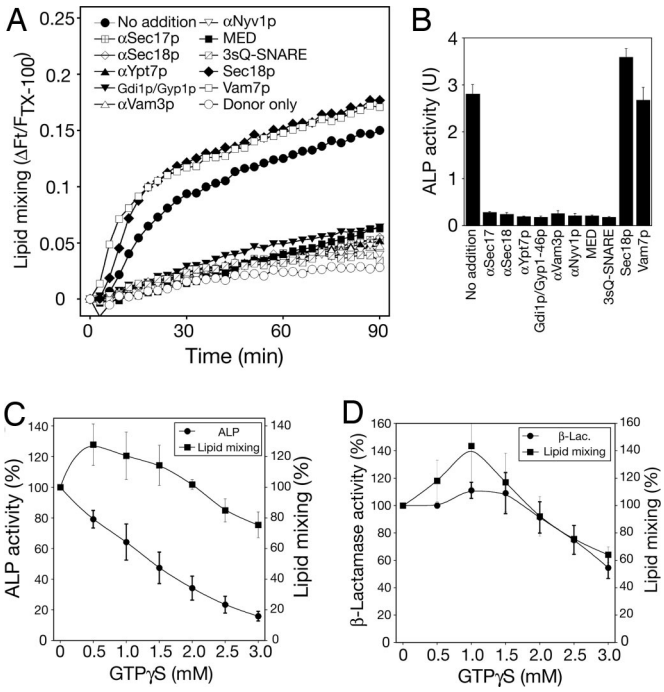

Fig. 3. The R18-dequenching lipid mixing assay. (*A*) Vacuoles were labeled with R18, mixed with unlabeled vacuoles in lipid mixing assay reactions containing anti-Sec17p (154 nM), anti-Sec18p (142 nM), anti-Ypt7p (167 nM), Gdi1p (1.2 μM)/Gyp1–46p (5 μM), anti-Vam3p (444 nM), anti-Nyv1p (261 nM), MED (10 μM), 3sQ-SNARE (2 μM), recombinant Sec18p (63 nM), rVam7p (40 nM), or buffer only (No addition), and lipid mixing was monitored at 27°C. One reaction did not receive unlabeled acceptor vacuoles (open circles). (*B*) After 90 min, ALP activity was measured. (*C* and *D*) Vacuoles isolated from BJ3505-Fos-ω were labeled with R18, reisolated, and added to lipid mixing assay reactions containing unlabeled DKY6281 vacuoles (*C*) or unlabeled vacuoles from BJ3505-α-Jun (*D*). Lipid mixing (squares) was monitored by R18 dequenching under low Mg^{2+} condition at 27°C for 90 min with the indicated concentrations of GTPγS. After 90 min, the reactions were assayed for ALP activity (*C*; circles) or β-lactamase activity (*D*; circles). Values obtained without inhibitors [2.31 ± 0.46 units for the ALP assay coupled with the R18 assay ($\Delta F_{90min}/F_{TX100}$ = 0.102 ± 0.047); 1.53 ± 0.07 units for the β-lactamase assay coupled with the R18 assay ($\Delta F_{90min}/F_{TX100}$ = 0.201 ± 0.023)] were used as the 100% reference. Data represent mean ± SEM (n = 3).

standard reaction of 772 scored (11%), and the same proportion, 118 of 1,190 scored (10%), acquired this size during incubation with 4 mM GTPγS, none acquired this size among either the 626 scored that had been incubated on ice without ATP or from the 1,127 scored that had been incubated with anti-Sec18 Fab. Thus, although high concentrations of GTPγS can inhibit fusion, GTPγS inhibition of the formation of active ALP is not a reliable indicator of fusion inhibition.

To assay lipid mixing between fusing vacuoles, vacuoles were labeled with self-quenching concentrations of octadecyl rhodamine B (R18). Fusion of R18-labeled donor vacuoles with unlabeled acceptor vacuoles permits dequenching through dilution of R18, as reported for rhodamine-phosphatidylethanolamine (PE) labeled vacuoles (9, 14). The increase in R18 fluorescence required unlabeled acceptor vacuoles (Fig. 3*A*, filled vs. open circles), was accelerated by recombinant Vam7p (open squares) or Sec18p (filled diamonds) and was blocked by priming inhibitors such as antibodies to Sec17p or Sec18p, Rab inhibitors including antibodies to Ypt7p and Gdi1p/Gyp1–46p, SNARE inhibitors such as a mixture of three soluble domains of vacuolar Q-SNAREs (15) and antibodies to Vam3p or Nyv1p or the phosphoinositide ligand MED, all of which inhibited the fusion in these same incubations (Fig. 3*B*). R18 has been extensively used in HA protein-mediated hemifusion studies (3–5, 16, 17). Because R18-dequenching during vacuole fusion requires unlabeled acceptor vacuoles, is sensitive to known fusion inhibitors, and can be stimulated by known fusion factors, it represents the authentic fusion pathway rather than R18 translocation (18) or fusion-independent R18 transfer. We compared the two content mixing assays, each coupled with the R18 dequenching assay, in the presence of GTPγS (Fig. 3 *C* and *D*). Low concentrations of GTPγS allowed or even stimulated lipid mixing (Fig. 3*C*, squares) while preventing the development of active ALP (circles), as reported (9). In contrast, when we assayed lipid and content mixing simultaneously by incubating R18-labeled BJ3505 vacuoles that contain Fos-ω with unlabeled BJ3505 vacuoles that contain α-Jun (Fig. 3*D*), GTPγS showed only modest and similar inhibition of both lipid mixing and content mixing. Differences in dequenching between these experiments (Fig. 3 *C* and *D*) may reflect that vacuoles from DKY6281 are only present in the ALP assay. We therefore sought other means of resolving the late stages of fusion.

To examine late reaction stages, docking can be synchronized. A portion of the membrane-anchored vacuole SNAREs is unpaired and ready to pair in trans, whereas Vam7p, which lacks

a transmembrane anchor, is present only on isolated vacuoles in *cis*-SNARE complexes (19). Its liberation by Sec17p/18p/ATP allows *trans*-SNARE complex assembly. By incubating vacuoles with anti-Sec17p antibodies (20, 21), tethering can occur, but *trans*-SNARE pairing is prevented by the absence of free Vam7p. Addition of soluble recombinant SNARE Vam7p (22) permits synchronous SNARE pairing (15). The reaction rapidly acquires insensitivity to Vam3p antibody (half-time <1 min), whereas content mixing occurs relatively slowly, with a half-time of 15 min (20, 21). Strikingly, after rVam7p addition the R18 dequenching (Fig. 4*A*, squares) has a half-time of ≈2 min, concurrent with or shortly after resistance to anti-Vam3p (diamonds) but well before content mixing (circles). Thus, lipid mixing occurs very soon after SNARE pairing but well before content mixing. We have recently shown that the phosphoinositide ligand MED prevents vacuole fusion, whereas it allows the formation of *trans*-SNARE complexes (23). We therefore assayed *trans*-SNARE complex formation (23), lipid mixing, and fusion from the same samples of mixed R18-labeled and unlabeled vacuoles. MED permits *trans*-SNARE pairing (Fig. 4*D*) but blocks lipid mixing (Fig. 4*B*) or fusion (Fig. 4*C*), suggesting that phosphoinositides are required for the rapid lipid mixing after *trans*-SNARE assembly.

The substantial lag in developing ALP activity could have been due to a slow proteolytic maturation of ALP. This is however unlikely: (*i*) Although the vacuolar protease Prb1p is largely responsible for ALP maturation, Prb1p overproduction has no effect on the kinetics of fusion-dependent ALP maturation (20), showing that Prb1p had not been limiting to maturation. (*ii*) Mature ALP appears *in vivo* with a half-life of 6 min (24), which includes its synthesis and transport through the endoplasmic reticulum and Golgi to the vacuole; thus the proteolytic maturation of pro-ALP in the vacuole takes much less than 6 min. (*iii*) The half-time of β-lactamase formation from its two halves in mixed detergent extracts of 0.2-mg vacuoles/ml from BJ3505-α-Jun and BJ3505-Fos-ω is ≈30 min (SI Fig. 5*B*), and with 2 mg/ml vacuole extracts the half-time for β-lactamase formation drops to 4 min (SI Fig. 5*D*); even these extracts have far lower concentrations of the two halves of β-lactamase than the intact and fused vacuoles. The kinetics of content mixing (fusion) in the ALP assay (SI Fig. 5*E*, open symbols) and β-lactamase assay (SI Fig. 5*E*, filled symbols) are identical, indicating that there is a true kinetic interval between the SNARE-pairing and lipid-mixing steps of docking and the final aqueous compartment mixing of fusion. This kinetic interval may reflect a lipidic, possibly hemifusion, intermediate during vacuole fusion, although we do not have direct evidence for hemifusion.

Discussion

We describe an assay that exploits the fusion-dependent reconstitution of β-lactamase activity from two complementary fragments. This complements the standard *in vitro* vacuole fusion assay of proteolytic activation of pro-Pho8p. The assay we describe has allowed a fresh evaluation of whether lipid mixing occurs at a distinct stage of fusion, such as a hemifusion intermediate, which precedes the final mixing of the aqueous vacuole lumens. Hemifusion was proposed as an intermediate during vacuole fusion based on the observation that GTPγS permitted lipid mixing but blocked the formation of active ALP (9). We now show that GTPγS is a more potent inhibitor of the formation of active ALP than of fusion *per se*, yet our findings are consistent with a hemifusion mechanism, as previously suggested (9). This sensitivity to GTPγS also vitiates our earlier use of this compound (25) in studies of the multiplicity of GTPases that regulate vacuole fusion.

Hemifusion can be induced in a minimal SNARE-driven liposome fusion system by low levels of wild-type SNARE proteins or by mutant SNARE proteins that have partial TMDs that only span the outer bilayer leaflet (6). A hemifusion intermediate was also detected at the single-liposome level by monitoring FRET between membrane-bound fluorophores in single fusion events between pairs of SNARE-reconstituted liposomes (7), and in flipped SNARE-mediated cell-cell fusion (8). These results suggest that the SNARE-dependent fusion of intracellular membranes like yeast vacuoles might also proceed through a hemifusion intermediate. We had previously reported that a reaction stage between docking and content mixing was sensitive to certain lipid ligands (19) and that lipid rearrangement is required after *trans*-SNARE complex formation before fusion (23), indicative of a lipidic intermediate. We now show that there is a substantial kinetic separation between lipid mixing and content mixing by using a R18-dequenching lipid-mixing assay and two distinct content-mixing assays.

What molecular models could encompass our current knowledge about vacuole lipid mixing and fusion? We have shown that proteins and lipids that are required for fusion become enriched at a vertex ring microdomain of docked vacuoles (26, 27). Fusion around this ring leaves membrane vesicles within the vacuole (27). This intralumenal membrane is not easily explained by a hemifusion model (SI Fig. 7*A*) in which an intermediate with a micron-sized hemifusion diaphragm proceeds to full fusion through a single fusion pore. We therefore propose a working model of vertex ring hemifusion to explain how a hemifusion intermediate can promote fusion around a vertex ring (SI Fig. 7*B*). Proteins and lipids that regulate docking and fusion accumulate at the vertex ring. The formation of *trans*-SNARE complexes around the ring may allow rapid lipid mixing between outer leaflets from two apposed bilayers (based on the similar kinetics of *trans*-SNARE complex formation and lipid mixing; Fig. 4*A*), generating a ring-shaped hemifusion diaphragm or a ring of point-hemifusions. This vertex ring hemifusion model fits better with key observations about vacuole fusion than a model (SI Fig. 7*A*) in which hemifusion originates at a single point on the apposed membrane surfaces (17). Three salient features of the latter model (SI Fig. 7*A*) are: (*i*) the absence of transmembrane proteins in the hemifusion diaphragm, (*ii*) the absence of external (cytoplasmic) leaflet lipids (SI Fig. 7*A*, green and red) in the hemifusion diaphragm, and (*iii*) the absence of a luminal vesicle after expansion of the fusion pore. Each of these features is difficult to reconcile with the observed facts of vacuole fusion: (*i*) the boundary membranes of docked vacuoles have a full complement of membrane proteins (27), and thus could not simply represent a large hemifusion diaphragm. (*ii*) FM4–64 and MDY-64, which label the external leaflet of vacuoles, are found with equal abundance in the boundary membrane microdomain as in the outer membrane (27). (*iii*) Fusion of docked vacuoles generates luminal vesicles bearing vacuolar lipids and integral membrane proteins (27). The vertex ring hemifusion model accommodates each of these observations; the boundary membrane consists of two complete bilayers and thus has integral membrane proteins and both bilayer leaflets. Current data do not distinguish between vertex ring hemifusion and a ring of point-hemifusion events. Resolution of the hemifused state by invasion of lipids, as shown in SI Fig. 7*B* (blue arrows in the middle panel), would generate luminal vesicles. Although this model may lead to further experiments, we caution that none of our results directly show hemifusion.

Classical hemifusion may represent a limiting condition of vertex ring hemifusion where the area of the apposed, boundary membrane approaches a point. Fusion studies of membranes bearing the HA protein (5) or SNAREs (28, 29) have suggested a ring of several copies of each protein around the nascent pore. Below a certain minimal size of the boundary membrane, a luminal vesicle would not form and point-hemifusion would be expected.

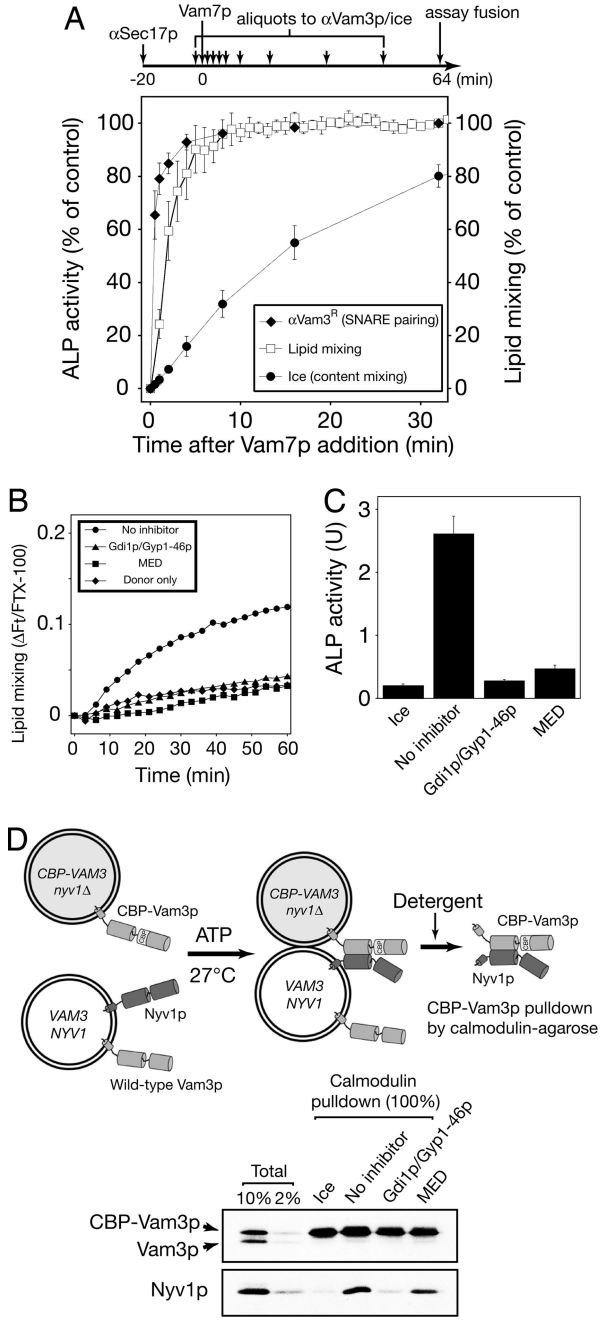

Fig. 4. Kinetics of lipid and content mixing. (*A*) Kinetic separation of SNARE complex assembly and lipid mixing from content mixing. ALP fusion reactions (1 μg of R18-labeled BJ3505 vacuoles and 5 μg of unlabeled DKY6281 vacuoles) contained affinity-purified anti-Sec17p (154 nM). Recombinant Vam7p (1 μM) was added after 20 min. A portion of each reaction was transferred to a microplate fluorometer and monitored for R18 dequenching at 27°C for 64 min. The remainder received anti-Vam3p IgG or were placed on ice at indicated times (−-0.5, 0.5, 1, 2, 4, 8, 16, 32, 48, or 64 min). ALP activity was measured after 64 min. Fusion values were normalized to reactions that were placed on ice at 64 min (3.48 ± 0.3). The relative fluorescence change $\Delta F_{64min}/F_{TX100}$ (see *Materials and Methods*) at 64 min (0.124 ± 0.002) was the 100% reference for lipid mixing. Data represent mean ± SEM ($n = 3$). (*B–D*) MED allows *trans*-SNARE complex assembly but blocks lipid mixing and content mixing. Vacuoles isolated from the BJ3505-CBP-Vam3p *nyv1*Δ yeast strain were labeled with 150 μM R18, reisolated, and added to lipid mixing assay reactions containing unlabeled vacuoles isolated from BJ3505-CBP-Vam3p *nyv1*Δ and DKY6281 yeast strains. The lipid mixing assay reactions (480 μl) contain 10.7 μg of R18-labeled vacuoles and 85.3 μg of unlabeled vacuoles. Lipid mixing was monitored at 27°C without inhibitors, with Gdi1p (1.2 μM)/Gyp1–46p (5 μM) or with MED (10 μM) (*B*). After 60 min, a portion of reactions (30 μl) was withdrawn to assay ALP activity (*C*). Data represent mean ± SEM ($n = 3$). The remaining reactions (450 μl) were subjected to assay of *trans*-SNARE complexes (see *Materials and Methods*). The transassociation of CBP-Vam3p from the BJ3505-CBP-Vam3p *nyv1*Δ vacuoles with Nyv1p from the DKY6281 vacuoles is shown (*D*).

Materials and Methods

Plasmids, Yeast Strains, and Reagents. The plasmid pYJ406 was generated by introducing the 720-bp upstream region and the 300-bp downstream region of the *ADH1* gene into XhoI/HindIII and SacII/SacI sites of the pRS406 plasmid. The pYJ406-CPY50 plasmid was constructed by ligating the first 50 codons of CPY into pYJ406, immediately 3′ of the *ADH1* promoter. Because the *ADH1* promoter is constitutively strong, and the N-terminal 50 aa of CPY can direct delivery of a fused protein to the vacuolar lumen (11), as confirmed with CPY50-YFP (data not shown), the resulting plasmid pYJ406-CPY50 allowed an overexpressed protein to be targeted to the vacuolar lumen. Plasmids Fos-GS-W and A-GS-Jun (10), generous gifts from Helen Blau (Stanford University, Stanford, CA), were used to amplify regions encoding a fusion protein of c-Fos α-helix and ω fragment of *E. coli* TEM1 β-lactamase and a chimera of α fragment of β-lactamase and c-Jun α-helix, respectively. The PCR products were subcloned into pYJ406-CPY50 by using BamHI and SacII sites, generating pYJ406-Fos-ω and pYJ406-α-Jun. Because the PCR product from A-GS-Jun has an internal BamHI site, BglII was used instead. Plasmids pYJ404-Fos-ω and pYJ404-α-Jun were also generated from pRS404 as above. Vacuoles from BJ3505 (*Matα ura3–52 trp1-Δ101 his3-Δ200 lys2-801 gal2 (gal3) can1 prb1-Δ1.6R pep4::HIS3*) (30) and DKY6281 (*Matα ura3-52 leu2-3,112 trp1-Δ901 his3-Δ200 lys2–801 suc2-Δ9 pho8::TRP1*) (13) were used for ALP fusion assays. To generate strains with Fos-ω and α-Jun in their vacuolar lumen, BJ3505 was transformed with pYJ406-Fos-ω and pYJ404-Fos-ω or pYJ406-α-Jun and pYJ404-α-Jun, generating BJ3505-Fos-ω or BJ3505-α-Jun. The resulting BJ3505-Fos-ω or BJ3505-α-Jun therefore bears two copies of Fos-ω or α-Jun, respectively. This double gene dosage yields a 2-fold-more-sensitive fusion assay. The vacuolar expression of the β-lactamase fragments was confirmed by immunoblotting (SI Fig. 5*A*). The β-lactamase substrate nitrocefin (Calbiochem, San Diego, CA) was dissolved in DMSO. GTPγS was purchased (Roche, Indianapolis, IN) as a 100 mM solution. Microcystin-LR (Alexis Biochemicals, San Diego, CA) and octadecyl rhodamine B (R18) (Molecular Probes, Eugene, OR) were dissolved in ethanol. MDY-64 (Molecular Probes) and the phospholipase C (PLC) inhibitor U73122 (Calbiochem) were dissolved in DMSO. Rabbit polyclonal antibody to β-lactamase was purchased from Chemicon International (Temecula, CA).

Vacuole Isolation and *in Vitro* ALP Fusion Assay. Vacuole concentrations were expressed as protein content, determined by Bradford with albumin standards. For the ALP assay, reactions (30 μl) contained 3 μg of vacuoles lacking the proteases Pep4p and Prb1p, 3 μg of vacuoles from cells without Pho8p, reaction buffer [125 mM KCl/5 mM $MgCl_2$/20 mM Pipes-KOH (pH 6.8)/200 mM sorbitol], 1 mM ATP, 40 mM creatine phosphate, 0.5 mg/ml creatine kinase, and 10 μM CoA (13). For experiments in the "low Mg^{2+}" condition, fusion reactions contained 0.25 mg/ml creatine kinase, 20 mM creatine phosphate, 0.5 mM ATP, and 0.5 mM $MgCl_2$ in reaction buffer [110 mM KCl/0.3 mM $MnCl_2$/200 mM sorbitol/10 mM Pipes/KOH (pH 6.8)] as described (9). After 90 min at 27°C, fusion was measured by assaying ALP.

The β-Lactamase Vacuole Fusion Assay. Vacuoles containing the chimeric protein Fos-ω or α-Jun were isolated from BJ3505-

Fos-ω or BJ3505-α-Jun (13). Standard β-lactamase fusion reactions (60 μl) contained 6 μg of vacuoles containing the fusion protein Fos-ω, 6 μg of vacuoles with α-Jun, the same reaction buffer, ATP, creatine phosphate, creatine kinase, and CoA as for the ALP fusion assay, and 11 μM recombinant GST-Fos protein (to reduce any background signal due to lysis). After 90 min at 27°C, the reactions were transferred to ice, 140 μl of ice-cold nitrocefin developing buffer [100 mM NaPi (pH 7.0)/150 μM nitrocefin/0.2% (vol/vol) Triton X-100] was added, and the mixture was placed in a 96-well clear plate with flat bottom (Corning Life Sciences, Corning, NY). Nitrocefin hydrolysis was measured by absorbance at 492 nm every 15 seconds for 5–10 min at 30°C with a VERSAmax microplate reader (Molecular Devices, Sunnyvale, CA); the absorbance increased linearly during this time interval, and the slope was determined. A blank reference well contained 150 μl from a sample containing 6 μg of Fos-ω vacuole, 6 μg of α-Jun vacuole, 11 μM recombinant GST-Fos protein, and 140 μl of nitrocefin developing buffer in 200 μl. One fusion unit of the β-lactamase fusion assay is defined as 1 nmol of hydrolyzed nitrocefin per minute from 12 μg of vacuole protein. One hundred nmol of hydrolyzed nitrocefin equals 0.53 of ΔOD_{492} (31).

Lipid Mixing Assay Using Octadecyl Rhodamine B (R18) Dequenching. Freshly prepared BJ3505 vacuoles (300 μg) were suspended in 400 μl of PS buffer containing 150 μM R18 in an amber microcentrifuge tube. After mixing gently with a wide-bore pipette tip, the mixture was incubated (10 min, 4°C) with rocking. PS buffer (600 μl) with 15% (wt/vol) Ficoll was added, and the suspension was transferred to a Polyallomer tube (11 × 60 mm) (Beckman, Fullerton, CA), overlaid with 1.2 ml of PS buffer with 8% (wt/vol) Ficoll, 1.2 ml of PS buffer with 4% (wt/vol) Ficoll, and 0.5 ml of PS buffer without Ficoll, centrifuged [20 min, 4°C, 105,200 × g, SW 60 Ti (Beckman)], and labeled vacuoles were recovered from the 0%/4%-Ficoll interface by using a wide-bore pipette tip. Standard lipid mixing assays (180 μl) contained 4 μg of R18-labeled vacuoles, 32 μg of unlabeled vacuoles, and the same reaction buffer, ATP, creatine phosphate, creatine kinase, and CoA as in fusion assays. Reaction mixtures (150 μl) were transferred to a 96-well flat-bottom assay plate with nonbinding surface (Corning). Fluorescence change was measured with a SpectraMax GeminiXPS fluorescent plate reader (Molecular Devices) at 27°C, 560-nm excitation and 590-nm emission as described (9) with minor modifications. Measurements were taken every 2–3 min for 60–90 min, yielding fluorescence values at the onset (F_0) and during the reaction (F_t). The final 10 measurements of a sample containing 0.33% (vol/vol) Triton X-100 was averaged and used as a value for the fluorescence after infinite dilution (F_{TX100}). The relative total fluorescence change $\Delta F_t/F_{TX100} = (F_t - F_0)/F_{TX100}$ was calculated. Fusion-dependent fluorescence change was calculated by subtracting fusion-independent fluorescence change values represented by a sample containing only labeled donor vacuoles from total fluorescence change values.

Assay of *trans*-SNARE Complexes. Assays of *trans*-SNARE complexes were performed as described (23) with modifications. Briefly, standard *trans*-SNARE and fusion assays (16×) contained 48 μg of vacuoles isolated from the BJ3505-CBP-Vam3p *nyv1*Δ yeast strain and 48 μg of vacuoles isolated from DKY6281 yeast strain. After 60 min, reactions were placed on ice (5 min). From each 16× reaction, 30 μl was withdrawn to assay Pho8p maturation, and the rest (450 μl) was centrifuged (11,000 × g, 5 min, 4°C). The supernatant was removed, and the sedimented vacuoles were overlaid with ice-cold solubilization buffer [200 μl of 20 mM TrisCl (pH 7.5)/150 mM NaCl/1 mM $MgCl_2$/0.5% Nonidet P-40 Alternative (Calbiochem)/10% glycerol/1× protease inhibitor mixture (0.46 μg/ml leupeptin/3.5 μg/ml pepstatin/2.4 μg/ml pefabloc-SC/1 mM PMSF], resuspended on ice, and solubilization buffer was added to a final volume of 600 μl. The extracts were mixed on a nutator rocker (20 min, 4°C), and the detergent insoluble material was removed by centrifugation (16,000 × g, 20 min, 4°C). Ten percent of the extract was removed for a total sample, and the remaining extract was brought to 2 mM $CaCl_2$. The CBP-Vam3p was recovered with calmodulin affinity beads (50 μl per 600 μl of extract; Stratagene, La Jolla, CA) on a nutator at 4°C overnight. Beads were collected by brief centrifugation (4,000 × g, 2 min, 4°C) and suspended five times with the solubilization buffer, followed by bead sedimentation. Bound proteins were eluted by boiling beads in SDS sample buffer containing 5 mM EGTA (94°C, 5 min) for SDS/PAGE analysis and immunoblotting.

We thank Dr. Helen Blau for reagents, Drs. Charles Barlowe and Ta Yuan Chang for suggestions, and Naomi Thorngren for excellent technical assistance. This work was supported by a grant from the National Institute of General Medical Sciences.

1. Cheever ML, Sato TK, de Beer T, Kutateladze TG, Emr SD, Overduin M (2001) *Nat Cell Biol* 3:613–618.
2. Stroupe C, Collins KM, Fratti RA, Wickner W (2006) *EMBO J* 25:1579–1589.
3. Kemble GW, Danieli T, White JM (1994) *Cell* 76:383–391.
4. Melikyan GB, White JM, Cohen FS (1995) *J Cell Biol* 131:679–691.
5. Chernomordik LV, Frolov VA, Leikina E, Bronk P, Zimmerberg J (1998) *J Cell Biol* 140:1369–1382.
6. Xu Y, Zhang F, Su Z, McNew JA, Shin YK (2005) *Nat Struct Mol Biol* 12:417–422.
7. Yoon TY, Okumus B, Zhang F, Shin YK, Ha T (2006) *Proc Natl Acad Sci USA* 103:19731–19736.
8. Giraudo CG, Hu C, You D, Slovic AM, Mosharov EV, Sulzer D, Melia TJ, Rothman JE (2005) *J Cell Biol* 170:249–260.
9. Reese C, Heise F, Mayer A (2005) *Nature* 436:410–414.
10. Wehrman T, Kleaveland B, Her JH, Balint RF, Blau HM (2002) *Proc Natl Acad Sci USA* 99:3469–3474.
11. Johnson LM, Bankaitis VA, Emr SD (1987) *Cell* 48:875–885.
12. Conradt B, Haas A, Wickner W (1994) *J Cell Biol* 126:99–110.
13. Haas A, Conradt B, Wickner W (1994) *J Cell Biol* 126:87–97.
14. Reese C, Mayer A (2005) *J Cell Biol* 171:981–990.
15. Jun Y, Thorngren N, Starai VJ, Fratti RA, Collins K, Wickner W (2006) *EMBO J* 25:5260–5269.
16. Chernomordik LV, Leikina E, Frolov V, Bronk P, Zimmerberg J (1997) *J Cell Biol* 136:81–93.
17. Melikyan GB, Brener SA, Ok DC, Cohen FS (1997) *J Cell Biol* 136:995–1005.
18. Melikyan GB, Deriy BN, Ok DC, Cohen FS (1996) *Biophys J* 71:2680–2691.
19. Collins KM, Thorngren NL, Fratti RA, Wickner WT (2005) *EMBO J* 24:1775–1786.
20. Merz AJ, Wickner WT (2004) *Proc Natl Acad Sci USA* 101:11548–11553.
21. Merz AJ, Wickner WT (2004) *J Cell Biol* 164:195–206.
22. Thorngren N, Collins KM, Fratti RA, Wickner W, Merz AJ (2004) *EMBO J* 23:2765–2776.
23. Collins KM, Wickner WT (2007) *Proc Natl Acad Sci USA* 104:8755–8760.
24. Klionsky DJ, Emr SD (1989) *EMBO J* 8:2241–2250.
25. Eitzen G, Will E, Gallwitz D, Haas A, Wickner W (2000) *EMBO J* 19:6713–6720.
26. Fratti RA, Jun Y, Merz AJ, Margolis N, Wickner W (2004) *J Cell Biol* 167:1087–1098.
27. Wang L, Seeley ES, Wickner W, Merz AJ (2002) *Cell* 108:357–369.
28. Cho SJ, Kelly M, Rognlien KT, Cho JA, Horber JK, Jena BP (2002) *Biophys J* 83:2522–2527.
29. Han X, Wang CT, Bai J, Chapman ER, Jackson MB (2004) *Science* 304:289–292.
30. Jones EW (2002) *Methods Enzymol* 351:127–150.
31. O'Callaghan CH, Morris A, Kirby SM, Shingler AH (1972) *Antimicrob Agents Chemother* 1:283–288.